Published OnlineFirst April 25, 2016; DOI: 10.1158/1535-7163.MCT-15-0938

Small Molecule Therapeutics

Molecular Cancer Therapeutics

The Discovery and Characterization of K-756, a Novel Wnt/β-Catenin Pathway Inhibitor Targeting Tankyrase

Ryoko Okada-Iwasaki[1,2], Yuichi Takahashi[1], Yasuo Watanabe[1], Hiroshi Ishida[1], Jun-ichi Saito[1], Ryuichiro Nakai[1], and Akira Asai[2]

Abstract

The Wnt/β-catenin pathway is a well-known oncogenic pathway. Its suppression has long been considered as an important challenge in treating cancer patients. Among colon cancer patients in particular, most patients carry an adenomatous polyposis coli (APC) mutation that leads to an aberration of Wnt/β-catenin pathway. To discover the small molecule inhibitors of the Wnt/β-catenin pathway, we conducted high-throughput screening in APC-mutant colon cancer DLD-1 cells using a transcriptional reporter assay, which identified a selective Wnt/β-catenin pathway inhibitor, K-756. K-756 stabilizes Axin and reduces active β-catenin, and inhibits the genes downstream of endogenous Wnt/β-catenin. We subsequently identified that K-756 is a tankyrase (TNKS) inhibitor. TNKS, which belongs to the PARP family, poly-ADP ribosylates Axin and promotes Axin degradation via the proteasome pathway. K-756 binds to the induced pocket of TNKS and inhibits its enzyme activity. Moreover, PARP family enzyme assays showed that K-756 is a selective TNKS inhibitor. K-756 inhibited the cell growth of APC-mutant colorectal cancer COLO 320DM and SW403 cells by inhibiting the Wnt/β-catenin pathway. An *in vivo* study showed that the oral administration of K-756 inhibited the Wnt/β-catenin pathway in colon cancer xenografts in mice. To further explore the therapeutic potential of K-756, we also evaluated the effects of K-756 in non–small cell lung cancer cells. Although a single treatment of K-756 did not induce antiproliferative activity, when K-756 was combined with an EGFR inhibitor (gefitinib), it showed a strong synergistic effect. Therefore, K-756, a novel selective TNKS inhibitor, could be a leading compound in the development of anticancer agents. *Mol Cancer Ther; 15(7); 1525–34. ©2016 AACR.*

Introduction

The Wnt/β-catenin pathway controls many biologic processes, including cell proliferation, stem cell renewal, and tissue development (1). When Wnt ligands bind to Frizzled (Frzd) receptors, a key downstream factor, β-catenin, localizes to the nucleus and forms a transcription complex with T-cell factor (TCF; ref. 2). The β-catenin/TCF complex switches on the downstream genes such as *MYC*, *BIRC5* (*SURVIVIN*), *FGF20*, *ASCL2*, *CEMIP* (*KIAA1199*), *VEGFA*, *DHRS9*, *CCND1*, *TNNC1*, and *AXIN2* (3–10). In contrast, when the Wnt ligand–mediated signaling is absent, β-catenin is degraded by a destruction complex, which is formed by adenomatous polyposis coli (APC), glycogen synthase kinase 3β (GSK3β), casein kinase (CK) 1α, and Axin (11).

The hyperactivation of the Wnt/β-catenin pathway is observed in many cancers including colon, gastric, and hepatocellular cancer (12, 13). The hyperactivation occurs due to the overexpression of the Wnt pathway–activating genes such as Wnt or β-catenin itself or a truncating mutation of the tumor suppressor APC, which is most often identified in colon cancer (12). APC deficiency leads to accumulation of nuclear β-catenin promoting the transcription of downstream target genes and leads to aberrant cell proliferation.

To develop an effective therapy for Wnt/β-catenin pathway deregulated cancer, many pharmacologic studies of small molecules and biologics have been attempted. Anti-Frizzled antibodies and porcupine inhibitors have already been studied in clinical trials (14, 15). These agents may be effective for cancers that exhibit deregulation of upstream factors such as Wnt overexpression. However, it would be difficult to render Wnt/β-catenin signaling with an APC mutation because APC-mutant cells do not depend on upstream Wnt signals for survival. In contrast, tankyrase (TNKS) inhibitor was discovered to inhibit Wnt/β-catenin signaling, even in APC-mutated cells (16). Therefore, TNKS has been considered to be an attractive target and several TNKS inhibitors have been discovered (16–18).

TNKS1 and 2 are members of the PARP family, which catalyze the modification of proteins using β-nicotinamide adenine dinucleotide (βNAD^+) as a substrate, resulting in the repeated addition of ADP-ribose to target proteins and the release of nicotinamide (19). TNKS was originally discovered as a factor in telomere maintenance. It poly-ADP ribosylate (PARsylate)s telomeric repeat binding factor 1 (TRF1) and controls the binding of TRF1 to telomeric DNA (19, 20). TNKS consists of three domains: a

[1]R&D Division, Kyowa Hakko Kirin Co., Ltd., Shizuoka, Japan. [2]Center for Drug Discovery, Graduate School of Pharmaceutical Sciences, University of Shizuoka, Shizuoka, Japan.

Note: Supplementary data for this article are available at Molecular Cancer Therapeutics Online (http://mct.aacrjournals.org/).

Corresponding Author: Ryuichiro Nakai, Kyowa Hakko Kirin Co., Ltd., 1188 Shimotogari, Nagaizumi-cho, Sunto-gun, Shizuoka 411-8731, Japan. Phone: 81-55-989-2004; Fax: 81-55-986-7430; E-mail: ryuichiro.nakai@kyowa-kirin.co.jp

doi: 10.1158/1535-7163.MCT-15-0938

Published OnlineFirst April 25, 2016; DOI: 10.1158/1535-7163.MCT-15-0938

catalytic PARP domain, the ankyrin (ANK) domain, and the sterile alpha module (SAM) domain. In the Wnt/β-catenin pathway, TNKS PARsylates Axin, leading to its ubiquitination by the ubiquitin E3 ligase RNF146, which results in Axin degradation by the proteasome complex (16, 21).

We herein report the discovery of a novel selective TNKS inhibitor, K-756, which was found to bind to an induced pocket of TNKS, and inhibit the Wnt/β-catenin pathway and cell growth in APC-mutant colon cancer cells. K-756 also induced a synergistic effect with gefitinib in EGFR-mutant non–small cell lung cancer (NSCLC) cells. Moreover, the oral administration of K-756 inhibited the Wnt/β-catenin pathway in a tumor xenograft model.

Materials and Methods

Cells and culture conditions

The human colon cancer cell line DLD-1 was obtained in 1998 from the Japanese Collection of Research Bioresources (Osaka, Japan). The COLO 320DM and SW403 human colon cancer cell lines were obtained in 2008 and 2012, respectively, from ATCC. The PC-9 human NSCLC cell line was obtained in 2006 from Immuno-Biological Laboratories (Gunma, Japan). The NCI-H322 human NSCLC cell line was obtained in 2007 from the European Collection of Cell Cultures. DLD-1 cells were grown in RPMI1640 with 10% FBS, 10 mmol/L HEPES, 1 mmol/L pyruvate solution, 4.5 mmol/L D-(+)-glucose solution, and 1% penicillin–streptomycin (PS; cat. no. 15140-122; Thermo Fisher Scientific). COLO 320DM cells, PC-9 cells, and NCI-H322 cells were grown in RPMI1640 with 10% FBS and 1% PS. SW403 cells were grown in DMEM high-glucose medium with 10% FBS and 1% PS. Cells were cultured at 37°C with 5% CO_2. All of the cell lines were authenticated by a short tandem repeat assay at the Japanese Collection of Research Bioresources.

Test and control articles

Nontargeting siRNA (sense: 5′-AUCCGCGCGAUAGUACGUAdTdT-3′, antisense: 5′-UACGUACUAUCGCGCGGAUdTdT-3′) and *CTNNB1* siRNA #1 (sense: 5′-CAGUUGUGGUUAAGCUCUUdAdC-3′, antisense: 5′-AAGAGCUUAACCACAACUGdTdT-3′) were custom synthesized and purified using an HPLC column by Gene Design (Osaka, Japan). Stealth nontargeting siRNA (#12935-113) and *CTNNB1* siRNA #2 (#HSS102462) were purchased from Thermo Fisher Scientific.

Reporter cell line

The DNA sequences, including the TCF-binding sites and the mutated TCF (mtTCF)-binding sites, were amplified from a TOPflash reporter plasmid (Millipore) and a FOPflash reporter plasmid (Millipore), respectively. The pGL4.27-TCF or pGL4.27-mtTCF plasmid was transfected into DLD-1 cells and hygromycin was added to the cells for stable cell line selection. A single clone with high reporter activity was selected for further experiments.

Reporter assay

DLD-1/TCF-Luc cells or DLD-1/mtTCF-Luc cells were seeded in 384-well white plates. The next day, the cells were treated with the compounds. After 18 hours, Steady Glo reagent (Promega) was added to the cells, and their luciferase activity was measured using a Top count NXT system (PerkinElmer).

Real-time reverse transcription-PCR

Cells were seeded in 24-well plates. The next day, the cells were treated with the compounds. After 24 hours, total RNA was extracted using an RNeasy Plus Kit (Qiagen) and reverse-transcribed using VILO reagent (Thermo Fisher Scientific). A real-time reverse transcription (RT)-PCR was performed with Platinum SYBR Green qPCR SuperMix-UDG (Thermo Fisher Scientific) or TaqMan Universal PCR Master Mix (Thermo Fisher Scientific). The transcript levels were determined using an ABI PRISM or Applied Biosystems 7500 Fast Real-Time PCR System (Thermo Fisher Scientific). Each mRNA level was normalized to the level of GAPDH mRNA. Correlation coefficients were calculated using the Microsoft Excel software program (Microsoft Corporation). The primers used for the real-time RT-PCR are shown below: *GAPDH* (sense primer: 5′-ACTTTGTCAAGCTCATTTCCTG-3′, anti-sense primer: 5′-CTCTCTTCCTCTTGTGCTCTTG-3′), *MYC* (sense primer: 5′-TTCGGGTAGTGGAAAACCAG-3′, antisense primer: 5′-CAGCAGCTCGAATTTCTTCC-3′), *BIRC5 (SURVIVIN)* (sense primer: 5′- GTTGCGCTTTCCTTTCTGTC-3′, antisense primer: 5′-GCACTTTCTTCGCAGTTTCC-3′), *FGF20* (TaqMan Assay ID: Hs00173929_m1), *ASCL2* (TaqMan Assay ID: Hs00270888_s1), *CEMIP (KIAA1199)* (TaqMan Assay ID: Hs00378530_m1), *VEGFA* (TaqMan Assay ID: Hs00900055_m1), *DHRS9* (TaqMan Assay ID: Hs00608375_m1), *GAPDH* (TaqMan Assay ID: Hs02758991_g1), *CCND1* (TaqMan Assay ID: Hs00765553_m1), *TNNC1* (TaqMan Assay ID: Hs00896999_g1), and *AXIN2* (TaqMan Assay ID: Hs00610344_m1).

Western blot analysis

The cells were seeded in 10-cm dishes. The next day, the cells were treated with compounds. After 24 hours, the cells were collected and lysed by NP40 lysis buffer (Thermo Fisher Scientific) with a protease inhibitor cocktail (Sigma-Aldrich). The lysate samples were prepared for equal protein concentration and Lane Marker Reducing Sample Buffer (5×; Thermo Fisher Scientific) was added. The samples were loaded onto SuperSep Ace gel (Wako Pure Chemical Industries) and separated by electrophoresis. The proteins were transferred to a polyvinylidene fluoride membrane using a semidry transfer apparatus. After the transfer, the membrane was blocked with 3% skim milk/TBS. After 30 minutes, the primary antibody was added to the membrane and incubated overnight at 4°C. The next day, the membranes were washed by TBS with 0.1% Tween-20 and the secondary antibody was added. The membranes were washed several times and added to Supersignal West Femto Maximum Sensitivity Substrate (Thermo Fisher Scientific). The targeted proteins were detected using an LAS4000 system (Fuji Film) or ABI600 (GE Healthcare). The following antibodies were used: anti-Axin1 antibody (Cell Signaling Technology), anti-Axin2 antibody (Cell Signaling Technology), anti-unphospho-β-catenin antibody (Millipore), anti-β-actin antibody (Sigma-Aldrich), anti-rabbit IgG, HRP-Linked F $(ab')_2$ fragment (Donkey; GE Healthcare), and anti-mouse IgG, HRP-linked F $(ab')_2$ fragment (Sheep; GE Healthcare).

TNKS and PARP family enzyme activity assay

The activity of each enzyme was measured using a PARP1, PARP2, PARP3, PARP6, PARP7, and PARP11 Chemiluminescent Assay Kit, and a TNKS1 and TNKS2 Histone Ribosylation Assay Kit (Antibody Detection) at BPS Bioscience. Enzymatic reactions were conducted in duplicate at 30°C for 1 hour in a 50 μL mixture containing an assay buffer, an enzyme-coated plate, and a

Published OnlineFirst April 25, 2016; DOI: 10.1158/1535-7163.MCT-15-0938

substrate. After the enzymatic reactions, 50 μL of streptavidin–HRP was added to each well and the plate was incubated at room temperature for an additional 30 minutes. One-hundred microliters of developer reagents was added to the wells and luminescence was measured using a BioTek Synergy2 microplate reader. The luminescence data were analyzed using the GraphPad Prism software program.

Crystallography

TNKS1 protein was purchased from CreLux. Apo TNKS1 crystals were obtained using the sitting drop vapor diffusion method by mixing the protein solution with an equal volume of reservoir solution containing 0.1 mol/L Na-Succinate pH 5.8 and 6% PEG MME 5,000. The complex crystals were obtained by soaking apo crystals for 18 hours in soaking buffer containing 0.1 mol/L Na-Succinate pH 5.8, 20% PEG MME 5,000, and 0.5 mmol/L K-756. The complex crystals were transferred to a cryoprotected solution containing 0.1 mol/L Na-Succinate pH 5.8, 30% PEG MME 5,000, and 0.5 mmol/L K-756 for flash cooling in liquid nitrogen before the diffraction experiments. The complex crystal belongs to the space group $P2_12_12$ with the following unit cell parameters: $a =$ 158.85 Å, $b = 74.68$ Å, $c = 84.60$ Å. The X-ray diffraction data for the complex crystal was collected at the BL5A beamline of Photon Factory in the High energy Accelerator Research Organization (Tsukuba, Japan). The data were processed using *HKL2000* (22). The structures were solved by molecular replacement using the *Phaser* program (23), and refined using the *Refmac5* program (24) from the *CCP4* software suite (25). The TNKS1 structure in complex with K-756 has been deposited in the Protein Data Bank with access codes 5ETY.

Cell viability and cell growth inhibition assays

For the cell viability assay, cells were seeded in 96-well white plates. siRNAs were reverse transfected by RNAiMax (Thermo Fisher Scientific). After 144 hours, a cell viability assay was performed using a Cell Titer-Glo Luminescent Cell Viability Assay Kit (Promega). Luciferase activity was measured using a Top count NXT system. For the cell growth inhibition assay, cells were seeded in 96-well plates. The next day, the cells were treated with the compounds. After 0, 72, or 144 hours of incubation, 2,3-bis[2-methoxy-4-nitro-S-sulfophenynl]H-tetrazolium-5 carboxanilide inner salt (XTT) reagent (Roche Diagnostics) was added to the cells. After 3 hours of incubation, the formation of formazan dye from tetrazolium salt XTT was measured using a SpectraMax 340PC system (Molecular Devices).

Analysis of the combination effects

The combination index (CI) was calculated using the Calcusyn software program (BIOSOFT), which was based on the combination index method of Chou and Talalay (26), using the data of the antiproliferative activity in cells treated with K-756, gefitinib, or a combination of the two compounds. Through this method, CI < 1 was defined as synergism and it indicated that CI in the range of 0.1 to 0.3 can be described as strong synergism (26).

Analysis of Wnt signaling in xenograft tumors

All animal studies were performed in accordance with the Standards for Proper Conduct of Animal Experiments at Kyowa Hakko Kirin Co., Ltd., under the approval of the company's Institutional Animal Care and Use Committee. K-756 was slowly suspended by 0.5% methylcellulose 400 solution (MC 400; Wako Pure Chemical Industries). SCID mice (CB17/Icr-Prkdc^{scid}/CrlCrlj, male, 5 weeks old) were obtained from Charles River Laboratories. The mice were subcutaneously implanted with 5×10^6 cells of DLD-1/TCF-Luc cells. After 13 days, the mice with a tumor volume of 236.38 to 595.80 mm^3 were divided into groups of 5 animals. On the day after grouping, 0.5% MC 400 or K-756 was orally administered to the mice once a day for 3 days. Twenty-four hours after the last administration of first and second day and 25 hours after the last administration of the third day, the tumor tissues were collected from the mice and frozen in liquid nitrogen. Tumor total RNA was extracted using an RNeasy mini Kit (Qiagen) and reverse-transcribed using VILO reagent (Thermo Fisher Scientific). An RT-PCR was performed as described before. Protein was extracted using a 10-fold dilution of the lysis buffer containing 1.5 g/L potassium dihydrogen phosphate (Nacalai tesque), 1 mL/L Triton X-100 (Sigma-Aldrich), 5 mol/L potassium hydroxide solution (Wako Pure Chemical Industries) at a pH of 7.8. After the protein assay, Bright Glo reagent (Promega) was added to the cells and luciferase activity was measured using a Top count NXT system. The values of *FGF20* and *LGR5* expression or luciferase activity were compared between the vehicle and compound-treated groups using a one-way ANOVA followed by a Dunnett test. Statistical analysis was carried out using Statistical Analysis System (SAS Institute).

Results

K-756 inhibits Wnt/β-catenin reporter activity in APC-mutant DLD-1 cells

We identified K-756 as a Wnt/β-catenin pathway small molecule inhibitor from high-throughput screening using a Wnt/β-catenin reporter assay in APC-mutant DLD-1 colon cancer cells. DLD-1 cells with a TCF reporter plasmid (DLD-1/TCF-Luc cells) and a mutant TCF reporter plasmid (DLD-1/mtTCF-Luc cells) were used for the primary and counter screening, respectively. The TCF and mutant TCF reporter plasmids were generated from TOPflash and FOPflash plasmids, which contains repeated TCF binding site (27). K-756 (Fig. 1A), which was synthesized at Kyowa Hakko Kirin as a quinazoline derivative (28), strongly inhibited the reporter activity in DLD-1/TCF-Luc cells with an IC_{50} of 110 nmol/L, but did not inhibit DLD-1/mtTCF-Luc cells, even at 1,000 nmol/L (Fig. 1C). On the contrary, K-050 (Fig. 1B), a close structural analogue of K-756 (29), did not inhibit the reporter activity in DLD-1/TCF-Luc cells or DLD-1/mtTCF-Luc cells (Fig. 1D). We, therefore, defined K-756 as a novel selective Wnt/β-catenin pathway reporter inhibitor.

The gene expression profile of K-756–treated cells downstream of Wnt/β-catenin is similar to that of *CTNNB1* siRNA-treated cells

Next, we compared the effect of *CTNNB1* siRNA and K-756 on the expression profiles of the genes downstream of Wnt/β-catenin to assess whether K-756 selectively inhibits the endogenous Wnt/β-catenin pathway. A certain expression profile was determined on the basis of the expression patterns of selected genes downstream of Wnt/β-catenin that were induced by a compound or a siRNA. If a gene expression profile of the compound-treated cells showed a high correlation with that of *CTNNB1* siRNA–treated cells, then the compound was considered to potentially be a selective Wnt/β-catenin inhibitor. As a

Published OnlineFirst April 25, 2016; DOI: 10.1158/1535-7163.MCT-15-0938

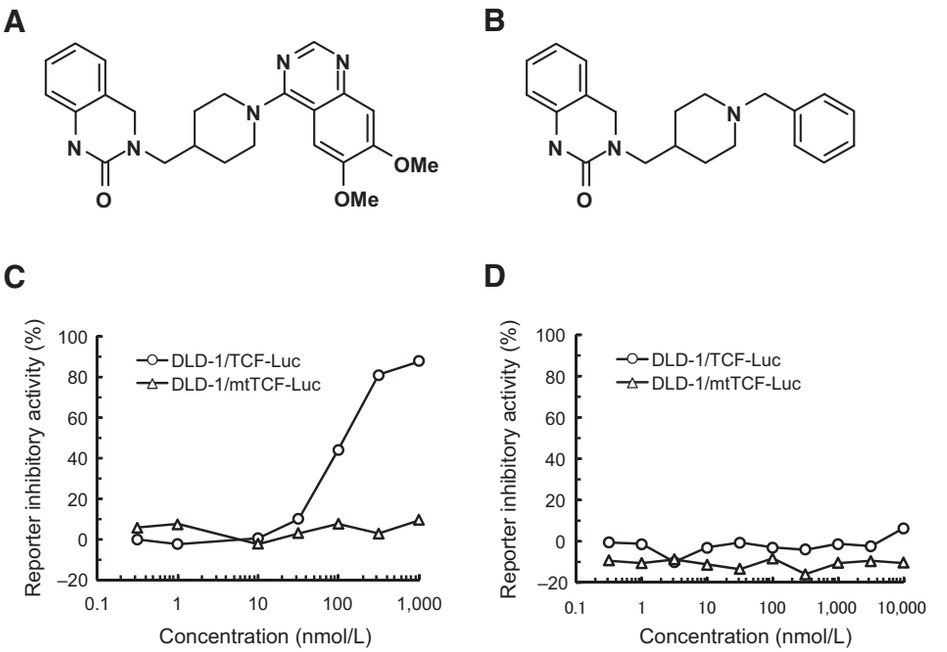

Figure 1.
The chemical structure and Wnt/β-catenin signaling inhibition by K-756. The chemical structures of K-756 (A) and K-050 (B), an inactive analogue. C, K-756 inhibited the reporter activity in DLD-1/TCF-Luc cells but not in DLD-1/mtTCF-Luc cells. DLD-1/TCF-Luc cells or DLD-1/mtTCF-Luc cells were treated with K-756; after 18 hours, their luciferase activity was measured. D, K-050 did not inhibit the reporter activity in DLD-1/TCF-Luc cells or in DLD-1/mtTCF-Luc cells. K-050 was added to the previously described cells. Each of the values represents the mean of triplicate experiments.

pilot experiment, the expression patterns of the genes downstream of Wnt/β-catenin were examined after *CTNNB1* siRNA treatment. DLD-1/TCF-Luc cells were transfected with two *CTNNB1* siRNAs with different targeted sequences. Both *CTNNB1* siRNAs showed sufficient *CTNNB1* knockdown at concentrations of 10 nmol/L (Supplementary Fig. S1A). The β-catenin protein was suppressed by 10 nmol/L of *CTNNB1* siRNAs (Supplementary Fig. S1B). Moreover, *CTNNB1* siRNA inhibited the reporter activity of DLD-1/TCF-Luc cells, whereas it did not inhibit that of DLD-1/mtTCF-Luc cells (Supplementary Fig. S1C). The mRNA levels of the genes downstream of the Wnt/β-catenin pathway (*MYC*, *ASCL2*, *DHRS9*, *FGF20*, *BIRC5*, *CEMIP*, and *VEGFA*) were measured by a real-time RT-PCR. As a result, the expression levels of all seven genes were found to have been altered by *CTNNB1* siRNA treatment (Supplementary Fig. S1D). The correlation coefficients among the gene expression profiles of the cells that were treated with *CTNNB1* siRNA#1 and *CTNNB1* siRNA#2 were above 0.92, which confirmed that the expression pattern of this gene set was appropriate as a profile of selective Wnt/β-catenin signaling inhibition (Supplementary Table S1). For reference, DLD-1/TCF-Luc cells were treated with XAV939 (3 μmol/L), a Wnt/β-catenin pathway inhibitor (16), to deduce its expression profile. The maximum correlation coefficient between the gene expression profile of the XAV939-treated cells and that of *CTNNB1* siRNA–treated cells was 0.80 (Supplementary Table S1). As a result, this correlation analysis, which was based on the selected gene set, proved an ideal way to identify selective Wnt/β-catenin inhibitors. K-756 inhibited the expression of the genes downstream of Wnt/β-catenin at concentrations that showed reporter inhibitory activity (Fig. 2A). The gene expression profile of K-756–treated cells showed a maximum correlation coefficient of 0.80 with *CTNNB1* siRNA–treated cells (Supplementary Table S1). K-756 was therefore defined as a selective Wnt/β-catenin pathway inhibitor.

K-756 stabilizes Axin1 and 2 by inhibiting TNKS1 and 2

Next, to examine the mechanism of action of K-756, DLD-1/TCF-Luc cells were treated with K-756 and the expression of Axin1, Axin2, and the unphosphorylated active form of β-catenin protein were detected by Western blot analysis. K-756 stabilized Axin1 and 2, and decreased active β-catenin in a dose-dependent manner (Fig. 2B). Huang and colleagues reported that a TNKS inhibitor, XAV939, stabilized Axin and promoted β-catenin protein degradation (16). We therefore assumed that K-756 also inhibits the enzymatic activity of TNKS. K-756 inhibited the ADP-ribosylation activity of TNKS1 and 2 with IC_{50}s of 31 and 36 nmol/L, respectively, confirming that K-756 is a direct inhibitor of TNKS (Fig. 2C). TNKS is one of the members of the PARP family (it is also known as PARP5). Therefore, our next concern was whether K-756 selectively inhibits TNKS among the other PARP family isoforms. To study the isoform selectivity of K-756, the PARP family enzyme inhibitory activity at 10 μmol/L was evaluated. K-756 inhibited TNKS1 and 2 by 97% and 100%, respectively (Table 1). In contrast, the inhibitory activity of K-756 against PARP 1, 2, 3, 6, 7, and 11 was less than 13%, whereas XAV939 inhibited PARP1 and 2 by 98% and 100%, respectively. Thus, K-756 was defined as a selective TNKS inhibitor.

K-756 binds to the induced pocket of TNKS1

The natural ligand of TNKS is β-NAD^+, which acts as a donor of ADP-ribose. TNKS catalyzes β-NAD^+ to transfer ADP-ribose moieties onto the target protein and releases nicotinamide (19, 30). Previous studies have identified two inhibitor binding pockets in TNKS: the nicotinamide-binding pocket and the induced pocket. For example, XAV939 has a nicotinamide-mimic moiety, which binds to the nicotinamide-binding pocket by forming a hydrogen bond interaction with Ser1221 and Gly1185 of TNKS1 (31). This binding mode is shared with other PARP family enzymes, thus XAV939 not only inhibits TNKS but also PARP1 and 2. In contrast, another TNKS inhibitor, IWR-1, binds to an induced pocket, which

Published OnlineFirst April 25, 2016; DOI: 10.1158/1535-7163.MCT-15-0938

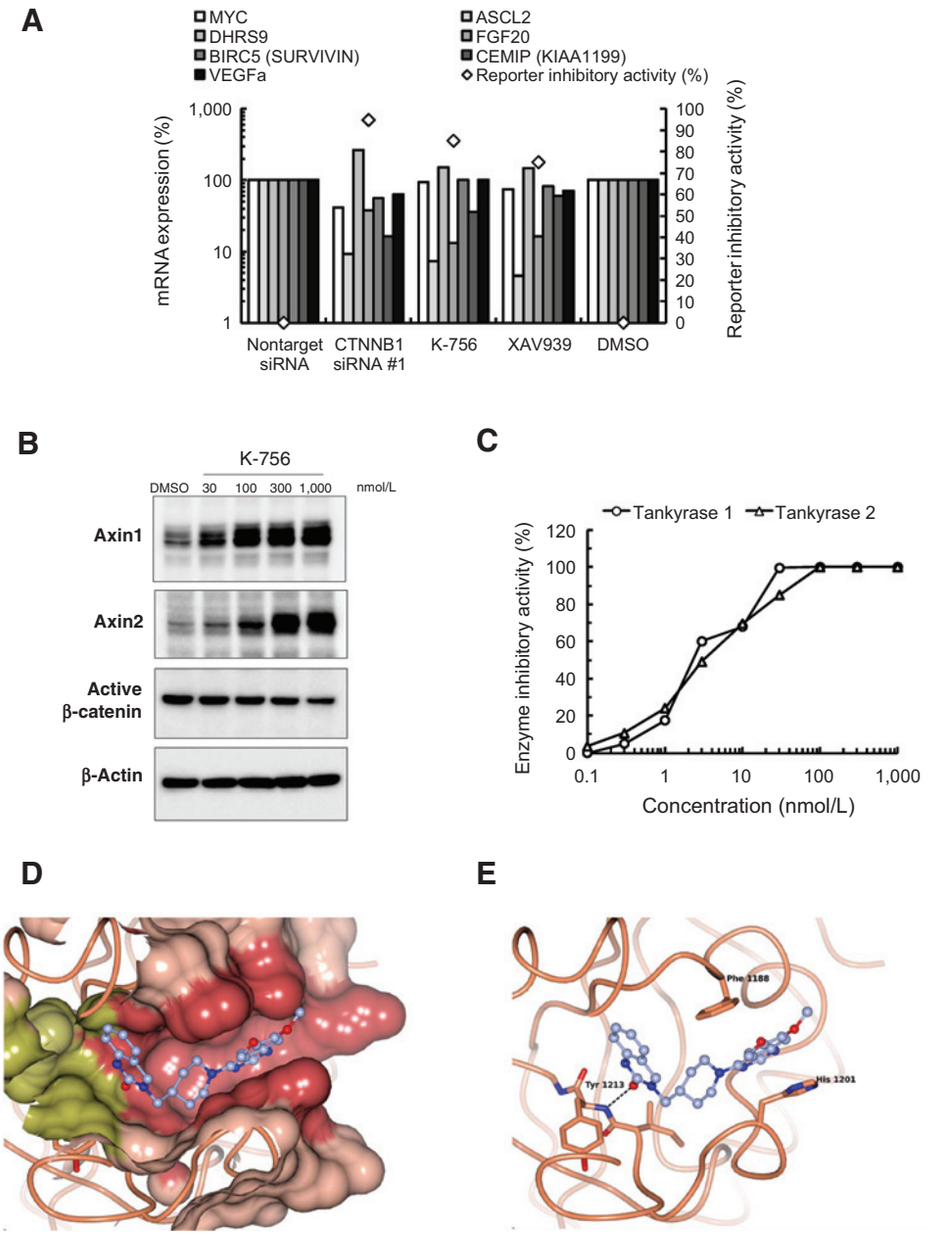

Figure 2.
K-756 regulates Wnt/β-catenin signaling by TNKS inhibition and binds to the induced pocket of TNKS1. A, the K-756–regulated Wnt/β-catenin downstream genes. The reporter inhibitory concentration of K-756 (10 μmol/L) or XAV939 (3 μmol/L) was added to DLD-1/TCF-Luc cells. After 24 hours, mRNA was collected and the expression levels of the Wnt/β-catenin downstream genes were measured by an RT-PCR. CTNNB1 siRNA#1 (1 nmol/L) was transfected to DLD-1/TCF-Luc cells. After 48 hours, mRNA was collected and an RT-PCR was performed. B, K-756 stabilized Axin1 and 2 and decreased the level of active β-catenin. K-756 was added to DLD-1/TCF-Luc cells. After 24 hours, the cells were collected and Western blot analysis was performed. C, K-756 inhibited TNKS1 and 2 enzyme activity. Each of the values represents the mean of duplicate experiments. D, the surface representation of the K-756 bound the induced pocket of TNKS1. The protein surface around the ligand binding pockets is shown in salmon pink. The induced pocket that K-756 binds is shown in red and the nicotinamide binding pocket is shown in gold. E, the interaction between K-756 and TNKS1. The Cα trace of the TNKS1 is shown with K-756, which is represented as ball-and-stick models with its carbon atoms shown in light blue. The residues involved in the interaction between K-756 and TNKS1 are shown as sticks. The hydrogen bond is shown as a dashed line.

is not present in the apo-TNKS structure (32, 33). This induced pocket is created by the drastic rearrangement of Phe1188 and is suggested to enable the nicotinamide noncompetitive inhibition of TNKS (33). To elucidate the binding mode of K-756, we analyzed the crystal structure of TNKS1 in combination with K-756 and found that K-756 bound to the induced pocket (Fig. 2D and E). The oxygen of the carbonyl group of quinazoline-2-one forms a hydrogen bond to the main chain NH of Tyr1213. This hydrogen bond interaction has been shown in other induced pocket binders (34). The 6′7′-dimethoxyquinozoline moiety is stacked with His1201, and the Phe1188 side chain contacts with one of two methoxy moieties. The stacking interaction of K-756 with His1201 coincides with its high selectivity to TNKS1 because this residue is only conserved in TNKS (and not in other PARP family enzymes; ref. 33).

Table 1. Inhibitory activity against PARP family enzymes

	Enzyme inhibitory activity (%) at 10 μmol/L							
Compound	**TNKS1**	**TNKS2**	**PARP1**	**PARP2**	**PARP3**	**PARP6**	**PARP7**	**PARP11**
K-756	97	100	8	1	0	7	13	3
XAV939	100	100	98	100	10	13	9	29
IWR-1	100	100	8	0	11	2	4	0

Published OnlineFirst April 25, 2016; DOI: 10.1158/1535-7163.MCT-15-0938

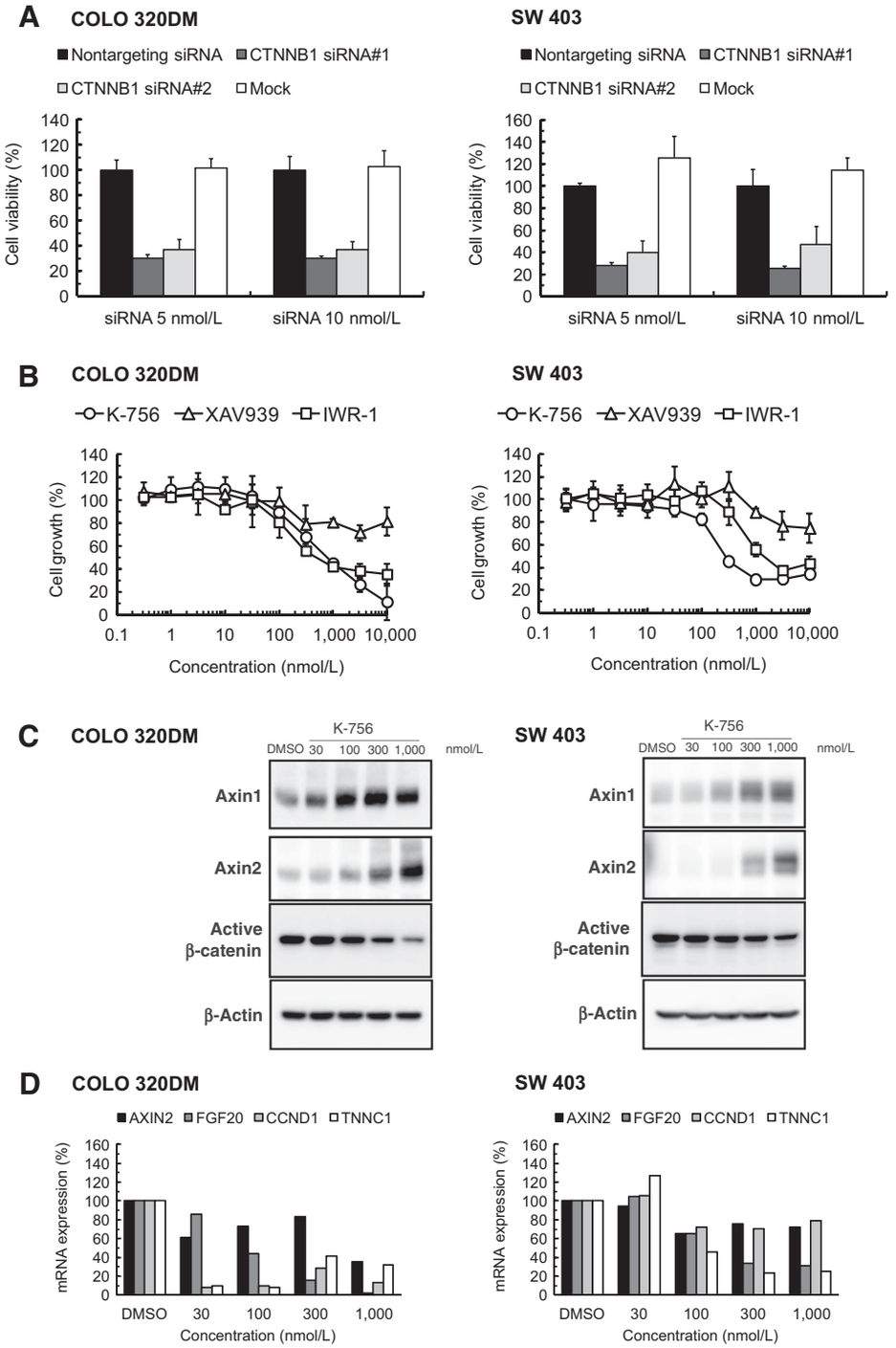

Figure 3.
K-756 inhibits Wnt/β-catenin signaling and the growth of Wnt/β-catenin pathway–dependent COLO 320DM and SW403 cells. A, *CTNNB1* siRNAs inhibited the cell growth of COLO 320DM and SW403 cells. *CTNNB1* siRNA#1 and #2 were transfected to COLO 320DM and SW403 cells in 96-well plates. Cell viability was measured after 144 hours. Each column represents the mean + SD of triplicate experiments. B, K-756 inhibited the cell growth of COLO 320DM and SW403 cells. K-756 was added to the cells in 96-well plates. After 144 hours, the antiproliferative activity was measured by an XTT assay. Each point represents the mean ± SD of triplicate experiments. C, K-756 stabilized Axin1 and 2 and decreased active β-catenin. K-756 was added to COLO 320DM and SW403 cells in 10-cm dishes. After 24 hours, cells were collected for Western blot analysis. D, K-756 inhibited the Wnt/β-catenin downstream genes. K-756 was added to COLO 320DM and SW403 cells in 24-well plates. After 24 hours, mRNA was collected for an RT-PCR.

K-756 inhibits the Wnt/β-catenin signaling and cell growth of Wnt/β-catenin–dependent APC-mutant colorectal cancer cell lines.

Although K-756 inhibited Wnt/β-catenin signaling in DLD-1/TCF-Luc cells, we did not observe clear cell growth inhibition in two-dimensional cultures (Supplementary Fig. S2A). When APC-mutant colorectal cancer cell line COLO 320DM and SW403 cells were transfected with *CTNNB1* siRNA and incubated for 144 hours, the cell viability of both cell lines decreased (Fig. 3A). As expected, the knockdown of the target gene was observed in both cell lines (Supplementary Fig. S2B). We therefore defined these cell lines as Wnt/β-catenin–dependent cell lines. The cells were treated with K-756 and after 144 hours, cell growth inhibition was measured by an XTT assay. The application of K-756 inhibited the cell growth of COLO 320DM with a GI_{50} of 780 nmol/L (Fig. 3B). K-050, an inactive analogue of K-756, did not inhibit the cell

Published OnlineFirst April 25, 2016; DOI: 10.1158/1535-7163.MCT-15-0938

growth of COLO 320DM (Supplementary Fig. S2C). K-756 also inhibited SW403 with a GI_{50} of 270 nmol/L (Fig. 3B). K-756 stabilized Axin1 and 2 and suppressed active β-catenin expression (Fig. 3C). It also downregulated the genes downstream of Wnt/β-catenin in both cell lines at a concentration that was consistent with cell growth inhibition (Fig. 3D). These results suggested that K-756 inhibited cell growth via Wnt/β-catenin inhibition. We also evaluated whether other TNKS inhibitors have equal effects. IWR-1 inhibited COLO 320DM cells with a GI_{50} of 410 nmol/L and SW403 cells with a GI_{50} of 1,300 nmol/L. XAV939 showed a moderate inhibition of less than 30%, even at a concentration of 10 μmol/L in both cells (Fig. 3B); however, both compounds inhibited DLD-1/TCF-Luc reporter activity with a similar potency (IC_{50}, IWR-1: 110 nmol/L; XAV939: 93 nmol/L; Supplementary Table S2) and stabilized Axins and suppressed active β-catenin after 24 hours of treatment in COLO 320DM and SW403 cells (Supplementary Fig. S3A and S3B). When the cells were cultured for long-term (72, 120, and 144 hours) with 1 μmol/L of K-756 and XAV939, the extent of Axin stabilization and active β-catenin inhibition level was lower in XAV939-treated cells compared with K-756–treated cells (Supplementary Fig. S3C). These results suggested that K-756 was more effective in inhibiting TNKS under long-term culture conditions. We did cell-cycle analysis of K-756 and IWR-1 in COLO 320DM cells and the compounds tended to increase G_2–M phase population in the cells (Supplementary Fig. S3D).

K-756 inhibits Wnt/β-catenin signaling in colon cancer cell xenografts in mice

To investigate whether K-756 inhibits Wnt/β-catenin signaling *in vivo*, we performed pharmacokinetic analysis in Balb/c mice. K-756 was administered orally at 1, 10, and 100 mg/kg, and after indicated time points plasma was collected and the plasma concentration of K-756 was analyzed. As a result, the plasma concentration at 100 mg/kg exceeded the plasma concentration converted IC_{50} of DLD-1/TCF-Luc cells for 7 hours (Supplementary Fig. S4A). As Wnt/β-catenin signal inhibition of K-756 was observed at 24 hours in the *in vitro* assays, we assumed that 100 mg/kg was not enough for full signal inhibition *in vivo*. Therefore, we decided to orally administer K-756 at 100, 200, and 400 mg/kg to detect *in vivo* Wnt/β-catenin signal inhibition in cancer cell xenograft mice. We created DLD-1/TCF-Luc cell xenografts in SCID mice. Vehicle (0.5% MC400) or K-756 was administered orally once a day for 3 days at 100, 200, and 400 mg/kg. The Wnt/β-catenin signal inhibition in the tumor was detected by measuring *FGF20* and *LGR5*, whose expressions were inhibited *in vitro* (Fig. 2A and Supplementary Fig. S4B), and luciferase activity. The expression of *FGF20* and reporter activity were significantly decreased at doses of 100 mg/kg and above at 3-day administration (Fig. 4A and C). The expression of *LGR5* was significantly decreased at doses of 200 mg/kg and above at 3-day administration (Fig. 4B). The maximum inhibitory activity was reached with the administration of K-756 at a dose of 400 mg/kg at 3-day administration (Fig. 4A–C). The Wnt/β-catenin signal inhibition at a dose of 400 mg/kg was observed from 1-day administration (Supplementary Fig. S4C–S4E).

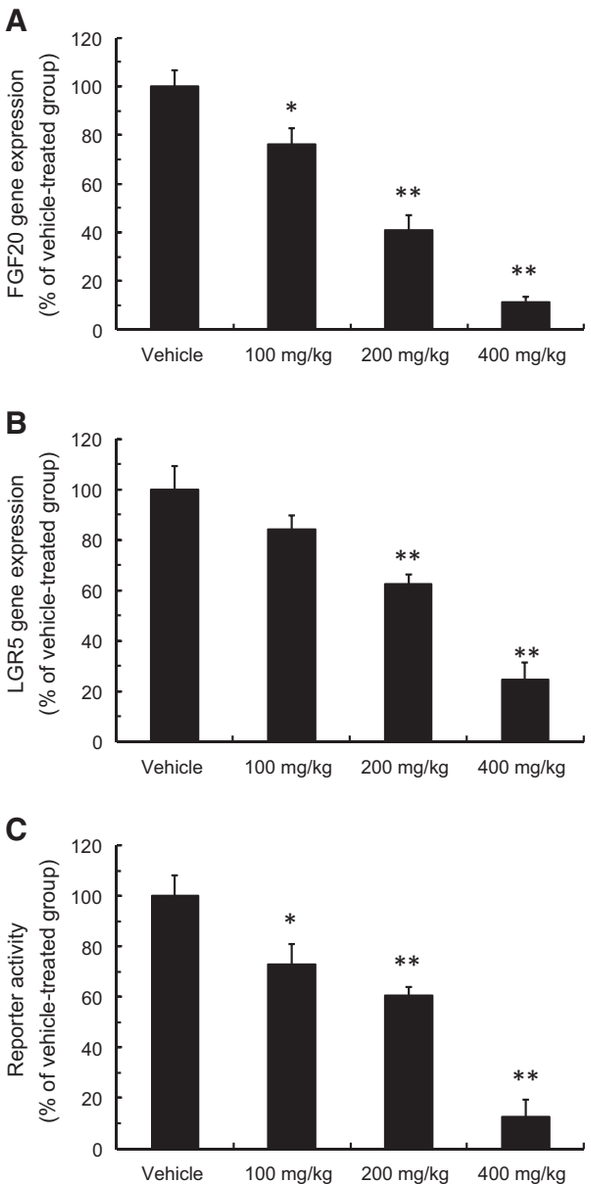

Figure 4.
K-756 inhibits Wnt/β-catenin signaling in DLD-1/TCF-Luc cell xenografts in mice. K-756 inhibited the *FGF20* (A) and *LGR5* expression (B) downstream of Wnt/β-catenin in DLD-1/TCF-Luc cell xenograft tumors. Mice were subcutaneously implanted with DLD-1/TCF-Luc cells. After 14 days, 0.5% MC 400 or K-756 was orally administered to the mice once a day for 3 days. Twenty-five hours after the last administration, the tumors were collected from the mice. RNA was extracted from the tumor; after mRNA extraction, RT-PCR was performed. Each column represents the mean + SE ($n = 5$); the asterisks indicate a statistically significant difference in comparison to the vehicle-treated group (*, $P < 0.05$; **, $P < 0.005$) in a one-way ANOVA followed by a Dunnett test. C, K-756 inhibited TCF-Luc reporter activity in DLD-1/TCF-Luc cell xenograft tumors. The tumors were prepared and collected as previously described. After protein lysis, a reporter assay was performed. Each column represents the mean + SE ($n = 5$).

K-756 shows a synergistic effect with gefitinib on cell viability in NSCLC cells

Casás-Selves and colleagues reported that TNKS shRNA showed a combination effect with an EGFR inhibitor (gefitinib) in NSCLC cells (35). We therefore studied the effect of K-756 combined with gefitinib on cell viability in EGFR exon 19-deletion mutant PC-9 cells (36) and wild-type EGFR NCI-H322 cells. After K-756 treatment, Axin1 was stabilized in PC-9 and NCI-H322 cells, indicating that TNKS was inhibited in the cells (Supplementary

Published OnlineFirst April 25, 2016; DOI: 10.1158/1535-7163.MCT-15-0938

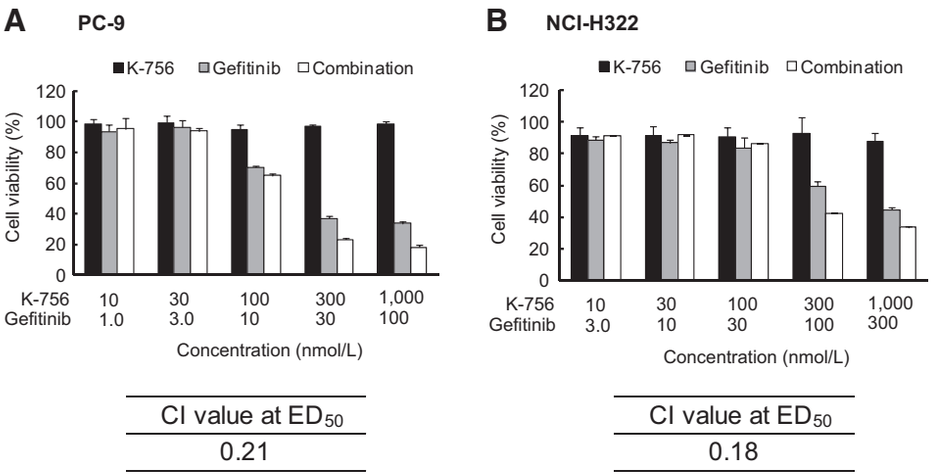

Figure 5.
The combination of K-756 and gefitinib showed synergistic growth inhibition in NSCLC cells. Cells were treated with K-756, gefitinib, or K-756 plus gefitinib for 72 hours, and cell viability was determined by an XTT assay. A, the results at a concentration ratio of 10:1 (K-756: gefitinib) in PC-9 cells; and B, at a concentration ration of 10:3 (K-756: gefitinib) in NCI-H322 cells are represented as percentages of viable cells in drug-treated cells relative to control cells. Each column represents the mean + SD of triplicate experiments. The CI values at ED_{50} are shown in the figure.

Fig. S5A). K-756 decreased active β-catenin in PC-9 cells but it did not clearly decrease in NCI-H322 cells. Thus, we detected Wnt/β-catenin downstream genes *DHRS9* and *CEMIP* and their expression levels were changed after K-756 treatment (Supplementary Fig. S5B). Therefore, we assumed that K-756 inhibited Wnt/β-catenin via TNKS inhibition in both PC-9 and NCI-H322 cells. To explore the effect of the combination of K-756 and gefitinib, cells were cotreated with K-756 and gefitinib for 72 hours. A single treatment of K-756 did not inhibit the cell viability of either of the cells. A single treatment of gefitinib inhibited both cell lines, while PC-9 cells showed higher sensitivity. Cotreatment of K-756 and gefinitib synergistically enhanced the cell death of PC-9 and NCI-H322 cells, in comparison with a single treatment of gefitinib (Fig. 5A and B). When PC-9 and NCI-H322 cells were cotreated with K-756 and gefitinib, the CI values at ED_{50} were 0.21 and 0.18, respectively. The data points with $0.1 < CI < 0.3$ describe the strong synergism of K-756 and gefitinib (26).

Discussion

Since the discovery of Wnt/β-catenin pathway regulation by TNKS, the development of TNKS inhibitors has gained much attention due to their potential use as cancer therapeutics (20). Several compounds with different structures and binding modes have been discovered to date (31, 34, 37). In this study, we discovered K-756 during the course of Wnt/β-catenin pathway reporter screening and a gene expression profile analysis (Figs. 1C and 2A). K-756 stabilized Axin1 and 2 and decreased active β-catenin (Fig. 2B), through a mechanism that was similar to that of a TNKS inhibitor, XAV939. An enzyme activity assay of TNKS (Fig. 2C) and a co-crystal structure analysis of TNKS1 with K-756 (Fig. 2D and E) identified K-756 as a novel TNKS inhibitor.

TNKS belongs to the PARP family; its natural ligand is β-NAD^+ (19). The TNKS inhibitor binds to two pockets: the nicotinamide pocket and the induced pocket (32). Nicotinamide pocket composing residues are conserved among the PARP family enzymes, including TNKS; thus, the nicotinamide pocket binders such as XAV939 show less selectivity to TNKS (16, 33). On the contrary, the induced pocket binders such as IWR-1 show high selectivity to TNKS due to the uniqueness of the pocket, which is only conserved in TNKS (33). The co-crystal structure of TNKS1 with K-756 revealed that K-756 binds to the induced pocket and that the 6′7′-dimethoxyquinozoline moiety of K-756 stacks with Phe1188 and His1201, which forms a hydrophobic pocket. K-050, an inactive analogue of K-756, lacks the 6′7′-dimethoxyquinozoline structure, thus its binding ability to TNKS is considered to be lost.

Because of its binding mode, K-756 showed high selectivity to TNKS among the other PARP family enzymes. PARP1/2 inhibitor was proven to be effective in the treatment of BRCA-mutated cancer patients; however, its side effects such as the induction of genome instability may be a matter of concern (38). Therefore, a highly selective TNKS inhibitor like K-756 may be a better candidate for the development of anticancer therapeutics than a less selective TNKS inhibitor like XAV939. Moreover, the results of our study suggested that the induced pocket binders such as K-756 and IWR-1 were more effective in inhibiting cell growth in long-term cultured cells. This might be due to their nicotinamide noncompetitive inhibition of TNKS.

In this study, we attempted to prove the concept of a TNKS inhibitor as an anticancer therapeutic agent. Unexpectedly, not all APC-mutated Wnt/β-catenin pathway–activated cells were susceptible to Wnt/β-catenin pathway inhibition. It was reported that XAV939 inhibited the colony formation of DLD-1 cells with a low serum condition (16). However, K-756 did not induce cell growth inhibition under our experimental conditions. COLO 320DM and SW403 cells were susceptible to *CTNNB1* siRNA, which indicates that the cell growth of these cell lines is dependent on the Wnt/β-catenin pathway (Fig. 3A). K-756 induced cell growth inhibition in these cell lines, which proved the antiproliferative activity of K-756 (Fig. 3B). The factors that define the susceptibility to TNKS inhibitors remain to be elucidated. Scholer-Dahirel and colleagues suggested that PI3K mutation status may define the Wnt/β-catenin dependency of colon cancer cells (39). Lau and colleagues suggested that the APC mutation status of colon cancer cells may define their sensitivity to a TNKS inhibitor (18). The verification of the factors that underlie the susceptibility to TNKS inhibitors will enable us to find a potential target segment for use as a monotherapy.

Combination treatment is an alternative strategy to find a potential target segment of TNKS inhibitors. K-756 was found to affect NSCLC cells when it was applied in combination with gefitinib. NSCLC accounts for 85% to 90% of lung cancer cases,

and the 5-year survival rate of patients with metastatic NSCLC remains low (40). Gefitinib, which is an EGFR inhibitor, is one of the treatment options for NSCLC patients; however, most patients relapse after treatment. A compound that synergizes with gefitinib might therefore make the treatment more durable and effective. K-756 showed a synergistic effect with gefitinib in both EGFR wild-type and mutant NSCLC cells (Fig. 5A and B). The synergistic effect of K-756 was seen at a concentration consistent with that which achieved Wnt/β-catenin signal inhibition. It has been demonstrated that *CTNNB1* siRNA also shows a synergistic effect with gefitinib (35). It is therefore assumed that this synergistic effect occurs due to Wnt/β-catenin inhibition. A TNKS inhibitor was also reported to show synergistic effects with a MEK inhibitor (18) and a PI3K/Akt inhibitor (41, 42). The mechanism underlying these combination effects may be due to crosstalk between the Wnt/β-catenin pathway and the EGFR, MAPK, or Akt pathways. A single treatment of a TNKS inhibitor may be effective in particular cancer cells whereas, when used in combination with other molecular targeted drugs, it may be effective for treating various types of cancer.

Not many TNKS inhibitors have been studied *in vivo*. XAV939 and IWR-1 are known to be metabolically unstable (43, 44).The most studied TNKS inhibitor is G007-LK; however, it was administered intraperitoneally (18). The oral administration of K-756 was effective in inhibiting the Wnt/β-catenin pathway in DLD-1/TCF-Luc cell xenografts in mice (Fig. 4A–C). As the Wnt/β-catenin pathway is also important in cancer cell differentiation (45) and antitumor immunity (46), future *in vivo* studies may reveal other effects of a TNKS inhibitor, which cannot be detected in *in vitro* studies. Also the intestinal toxicity, which was observed with G007-LK, should be studied with other chemotypes to see if it is an on-target effect of TNKS inhibition. Collectively, an orally administrable and selective compound such as K-756 could be a valuable lead compound for further development of more potent derivatives, which is expected to be an anticancer therapeutic.

Disclosure of Potential Conflicts of Interest

No potential conflicts of interest were disclosed.

Authors' Contributions

Conception and design: R. Okada-Iwasaki, Y. Watanabe, H. Ishida, R. Nakai, A. Asai

Development of methodology: R. Okada-Iwasaki, Y. Watanabe, R. Nakai

Acquisition of data (provided animals, acquired and managed patients, provided facilities, etc.): R. Okada-Iwasaki, Y. Takahashi, Y. Watanabe, H. Ishida

Analysis and interpretation of data (e.g., statistical analysis, biostatistics, computational analysis): R. Okada-Iwasaki, Y. Takahashi, Y. Watanabe, J.-i. Saito, R. Nakai

Writing, review, and/or revision of the manuscript: R. Okada-Iwasaki, Y. Takahashi, Y. Watanabe, H. Ishida, R. Nakai, A. Asai

Administrative, technical, or material support (i.e., reporting or organizing data, constructing databases): R. Okada-Iwasaki, Y. Watanabe, H. Ishida

Study supervision: J.-i. Saito, R. Nakai, A. Asai

Acknowledgments

The authors thank Mr. Michihiko Suzuki and Mr. Kazuki Asanome for their interest and support of this study.

Grant Support

This work was supported by Kyowa Hakko Kirin Co. Ltd.

The costs of publication of this article were defrayed in part by the payment of page charges. This article must therefore be hereby marked *advertisement* in accordance with 18 U.S.C. Section 1734 solely to indicate this fact.

Received December 7, 2015; revised April 7, 2016; accepted April 9, 2016; published OnlineFirst April 25, 2016.

References

1. Clevers H. Wnt/β-catenin signaling in development and disease. Cell 2006;127:469–80.
2. van Noort M, Clevers H. TCF transcription factors, mediators of Wnt-signaling in development and cancer. Dev Biol 2002;244:1–8.
3. He TC, Sparks AB, Rago C, Hermeking H, Zawel L, da Costa LT, et al. Identification of c-MYC as a target of the APC pathway. Science 1998;281:1509–12.
4. Kim PJ, Plescia J, Clevers H, Fearon ER, Altieri DC. Survivin and molecular pathogenesis of colorectal cancer. Lancet 2003;362:205–9.
5. Chamorro MN, Schwartz DR, Vonica A, Brivanlou AH, Cho KR, Varmus HE. FGF-20 and DKK1 are transcriptional targets of beta-catenin and FGF-20 is implicated in cancer and development. EMBO J 2005;24:73–84.
6. Jubb AM, Chalasani S, Frantz GD, Smits R, Grabsch HI, Kavi V, et al. Achaete-scute like 2 (ascl2) is a target of Wnt signalling and is upregulated in intestinal neoplasia. Oncogene 2006;25:3445–57.
7. Birkenkamp-Demtroder K, Maghnouj A, Mansilla F, Thorsen K, Andersen CL, Øster B, et al. Repression of KIAA1199 attenuates Wnt-signalling and decreases the proliferation of colon cancer cells. Br J Cancer 2011;105:552–61.
8. Zhang X, Gaspard JP, Chung DC. Regulation of Vascular Endothelial Growth Factor by the Wnt and K-ras pathways in colonic neoplasia. Cancer Res 2001;61:6050–4.
9. Nadauld LD, Phelps R, Moore BC, Eisinger A, Sandoval IT, Chidester S, et al. Adenomatous polyposis coli control of C-terminal binding protein-1 stability regulates expression of intestinal retinol dehydrogenases. J Biol Chem 2006;281:37828–35.
10. Shtutman M, Zhurinsky J, Simcha I, Albanese C, D'Amico M, Pestell R, et al. The cyclin D1 gene is a target of the β-catenin/LEF-1 pathway. Proc Natl Acad Sci 1999;96:5522–7.
11. Kimelman D, Xu W. Beta-catenin destruction complex: Insights and questions from a structural perspective. Oncogene 2006;25:7482–91.
12. Polakis P. Wnt signaling and cancer. Genes Dev 2000;14:1837–51.
13. Klaus A, Birchmeier W. Wnt signalling and its impact on development and cancer. Nat Rev Cancer 2008;8:387–98.
14. Gurney A, Axelrod F, Bond CJ, Cain J, Chartier C, Donigan L, et al. Wnt pathway inhibition via the targeting of Frizzled receptors results in decreased growth and tumorigenicity of human tumors. Proc Natl Acad Sci 2012;109:11717–22.
15. Liu J, Pan S, Hsieh MH, Ng N, Sun F, Wang T, et al. Targeting Wnt-driven cancer through the inhibition of porcupine by LGK974. Proc Natl Acad Sci 2013;110:20224–9.
16. Huang S-MA, Mishina YM, Liu S, Cheung A, Stegmeier F, Michaud GA, et al. Tankyrase inhibition stabilizes axin and antagonizes Wnt signalling. Nature 2009;461:614–20.
17. Chen B, Dodge ME, Tang W, Lu J, Ma Z, Fan C-W, et al. Small molecule–mediated disruption of Wnt-dependent signaling in tissue regeneration and cancer. Nat Chem Biol 2009;5:100–7.
18. Lau T, Chan E, Callow M, Waaler J, Boggs J, Blake RA, et al. A novel tankyrase small-molecule inhibitor suppresses APC mutation-driven colorectal tumor growth. Cancer Res 2013;73:3132–44.
19. Smith S, Giriat I, Schmitt A, de Lange T. Tankyrase, a poly(ADP-ribose) polymerase at human telomeres. Science 1998;282:1484–7.
20. Riffell JL, Lord CJ, Ashworth A. Tankyrase-targeted therapeutics: expanding opportunities in the PARP family. Nat Rev Drug Discov 2012;11:923–36.
21. Callow MG, Tran H, Phu L, Lau T, Lee J, Sandoval WN, et al. Ubiquitin ligase RNF146 regulates tankyrase and Axin to promote Wnt signaling. PLoS One 2011;6:e22595.
22. Otwinowski Z, Minor W. Processing of X-ray diffraction data collected in oscillation mode. Methods Enzymol 1997;276:307–26.
23. McCoy AJ, Grosse-Kunstleve RW, Adams PD, Winn MD, Storoni LC, Read RJ. Phaser crystallographic software. J Appl Crystallogr 2007;40:658–74.

24. Murshudov GN, Skubák P, Lebedev AA, Pannu NS, Steiner RA, Nicholls RA, et al. REFMAC 5 for the refinement of macromolecular crystal structures. Acta Crystallogr Sect D Biol Crystallogr 2011;67:355–67.
25. Collaborative Computational Project, Number 4. The CCP4 suite: programs for protein crystallography. Acta Crystallogr Sect D Biol Crystallogr 1994;50:760–3.
26. Chou T-C. Theoretical basis, experimental design, and computerized simulation of synergism and antagonism in drug combination studies. Pharmacol Rev 2006;58:621–81.
27. Korinek V, Barker NJ, Morin P, van Wichen D, Vogelstein B, Clevers H, et al. Constitutive transcriptional activation by a beta-Catenin-Tcf complex in $APC^{-/-}$ colon carcinoma. Science 1997;275:1784–7.
28. Nomoto Y, Obase H, Takai H, Hirata T, Teranishi M, Nakamura J, et al. Studies on cardiotonic agents. I. Synthesis of some quinazoline derivatives. Chem Pharm Bull 1990;38:1591–5.
29. Takai H, Obase H, Teranishi M, Karasawa A, Kubo K, Shuto K, et al. Synthesis of piperidine derivatives with a quinazoline ring system as potential antihypertensive agents. Chem Pharm Bull 1986;34:1907–16.
30. Shultz MD, Kirby CA, Stams T, Chin DN, Blank J, Charlat O, et al. [1,2,4]Triazol-3-ylsulfanylmethyl-3-phenyl-[1,2,4]oxadiazoles: antagonists of the Wnt pathway that inhibit tankyrases 1 and 2 via novel adenosine pocket binding. J Med Chem 2012;55:1127–36.
31. Bregman H, Gunaydin H, Gu Y, Schneider S, Wilson C, Dimauro EF, et al. Discovery of a class of novel tankyrase inhibitors that bind to both the nicotinamide pocket and the induced pocket. J Med Chem 2013;56:1341–5.
32. Narwal M, Venkannagari H, Lehtiö L. Structural basis of selective inhibition of human tankyrases. J Med Chem 2012;55:1360–7.
33. Gunaydin H, Gu Y, Huang X. Novel binding mode of a potent and selective tankyrase inhibitor. PLoS One 2012;7:e33740.
34. Hua Z, Bregman H, Buchanan JL, Chakka N, Guzman-Perez A, Gunaydin H, et al. Development of novel dual binders as potent, selective, and orally bioavailable tankyrase inhibitors. J Med Chem 2013;56:10003–15.
35. Casas-Selves M, Kim J, Zhang Z, Helfrich BA, Gao D, Porter CC, et al. Tankyrase and the canonical Wnt pathway protect lung cancer cells from EGFR inhibition. Cancer Res 2012;72:4154–64.
36. Ogino A, Kitao H, Hirano S, Uchida A, Ishiai M, Kozuki T, et al. Emergence of Epidermal Growth Factor Receptor T790M mutation during chronic exposure to Gefitinib in a non small cell lung cancer cell line. Cancer Res 2007;67:7807–14.
37. Wahlberg E, Karlberg T, Kouznetsova E, Markova N, Macchiarulo A, Thorsell A-G, et al. Family-wide chemical profiling and structural analysis of PARP and tankyrase inhibitors. Nat Biotechnol 2012;30:283–8.
38. Wang Z-Q, Stingl L, Morrison C, Jantsch M, Los M, Schulze-Osthoff K, et al. PARP is important for genomic stability but dispensable in apoptosis. Genes Dev 1997;11:2347–58.
39. Scholer-Dahirel A, Schlabach MR, Loo A, Bagdasarian L, Meyer R, Guo R, et al. Maintenance of adenomatous polyposis coli (APC)-mutant colorectal cancer is dependent on Wnt/β-catenin signaling. Proc Natl Acad Sci 2011;108:17135–40.
40. Reck M, Popat S, Reinmuth N, De Ruysscher D, Kerr KM, Peters S. Metastatic non-small-cell lung cancer (NSCLC): ESMO Clinical Practice Guidelines for diagnosis, treatment and follow-up. Ann Oncol 2014;25: iii27–iii39.
41. Tenbaum SP, Ordóñez-Morán P, Puig I, Chicote I, Arqués O, Landolfi S, et al. β-catenin confers resistance to PI3K and AKT inhibitors and subverts FOXO3a to promote metastasis in colon cancer. Nat Med 2012;18: 892–901.
42. Arques O, Chicote I, Puig I, Tenbaum SP, Argiles G, Dienstmann R, et al. Tankyrase inhibition blocks Wnt/β-catenin pathway and reverts resistance to PI3K and AKT inhibitors in the treatment of colorectal cancer. Clin Cancer Res 2016;22:644–56.
43. Shultz MD, Cheung AK, Kirby CA, Firestone B, Fan J, Chen CH-T, et al. Identification of NVP-TNKS656: The use of structure–efficiency relationships to generate a highly potent, selective, and orally active tankyrase inhibitor. J Med Chem 2013;56:6495–511.
44. Lu J, Ma Z, Hsieh JC, Fan CW, Chen B, Longgood JC, et al. Structure-activity relationship studies of small-molecule inhibitors of Wnt response. Bioorganic Med Chem Lett 2009;19:3825–7.
45. Dow LE, O'Rourke KP, Simon J, Tschaharganeh DF, van Es JH, Clevers H, et al. Apc restoration promotes cellular differentiation and reestablishes crypt homeostasis in colorectal cancer. Cell 2015;161: 1539–52.
46. Spranger S, Bao R, Gajewski TF. Melanoma-intrinsic β-catenin signalling prevents anti-tumour immunity. Nature 2015;523:231–5.

Published OnlineFirst April 25, 2016; DOI: 10.1158/1535-7163.MCT-15-0938

AACR American Association for Cancer Research

Molecular Cancer Therapeutics

The Discovery and Characterization of K-756, a Novel Wnt/β-Catenin Pathway Inhibitor Targeting Tankyrase

Ryoko Okada-Iwasaki, Yuichi Takahashi, Yasuo Watanabe, et al.

Mol Cancer Ther 2016;15:1525-1534. Published OnlineFirst April 25, 2016.